BULLETIN OF THE EARTHQUAKE
RESEARCH INSTITUTE
Vol. 46 (1968), pp. 1075-1102

52. The Westward Drift of the Geomagnetic Secular Variation.

By Takesi YUKUTAKE and Hiroko TACHINAKA,

Earthquake Research Institute.

(Read June 18, 1968.—Received July 9, 1968.)

Summary

It is shown that sufficiently reliable coefficients of spherical harmonic series for the geomagnetic secular change are obtainable by comparison of spherical harmonic coefficients of the main field for different epochs spaced at fairly long intervals. Then the spherical harmonic coefficients of the secular change $\dot{g}_n^m$ and $\dot{h}_n^m$ are computed for the epochs 1806, 1857 and 1900, and synthesized to obtain isoporic charts of the non-dipole field.

The isoporic charts thus synthesized indicate that the westward drift is the most prevailing feature of the geomagnetic secular variation, in contrast to the non-dipole anomalies most of which remain at the same position and only a few drift westwards. The result that the whole distribution of the secular change drifts westward suggests that the drifting part of the non-dipole field has global distribution as well as the standing part. It is probably due to the predominant standing anomalies which conceal most parts of the drifting anomalies that only a few of the anomalies can be recognized to be drifting.

Poleward shift of the isoporic foci was also noted, but it seems to be associated with a rapid growth of an equatorial zone where the change in the vertical force is negative.

1. Introduction

The earth's magnetic field is roughly that of a dipole. When the dipole field is removed from the observed field, several large regional anomalies of continental size which is called the non-dipole field cover the whole surface of the earth. Until recent times, it had been widely believed that most parts of the non-dipole field drift westwards uniformly as a whole[1),2)]. However, an examination of the non-dipole field

1) E. C. BULLARD, C. FREEDMAN, H. GELLMAN and J. NIXON, "The Westward Drift of the Earth's Magnetic Field" *Phil. Trans. Roy. Soc. London*, A, **234** (1950), 67-92.

2) T. YUKUTAKE, "The Westward Drift of the Magnetic Field of the Earth," *Bull. Earthq. Res. Inst.*, **40** (1962), 1-65.

during the last several hundred years revealed that many of the non-dipole anomalies had remained still nearly at the same position and that only a few anomalies travelled westwards[3]. The result is concordant, on one hand, with a few investigations which suggest that there is a local fluctuation in the drift velocity. Examining recent magnetic maps, Whitham could not find any marked tendency of westward drift of the magnetic field in Canada[4]. Yukutake noticed that the westward drift velocity is small in the Pacific area compared with the world average[5]. Pochtarev noted that many of the large regional anomalies do not show any appreciable movement since 1885[6]. However, the result also seems seriously discordant with some other observations. When archeomagnetic data and old instrumental observations are examined at various places, the maximum deviations of the magnetic declination and the maxima or the minima of the inclination have been drifting clearly with a mean rate of 0.36°/year during the past thousand years[7].

The previous work on the non-dipole field which showed that most of the anomalies were standing ones does not absolutely exclude the possibility of worldwide drifting of the geomagnetic field. When the intensities of the standing anomalias are far stronger than those of drifting ones, the effect of drifting on the entire distribution of the non-dipole field may hardly be detected, even if the drifting field has worldwide distribution. In this paper it is attempted to examine whether the drifting parts are really restricted to a few localized regions or that the predominant standing anomalies mask the main parts of the drifting anomalies and only a few conspicuous features are recognized to drift.

If the intensity of the standing anomaly does not vary with time, the observed rate of change in the field is entirely due to the drifting anomalies and the whole distribution of the secular change is expected to exhibit drifting. From this view point, time variations in the geomagnetic secular change are examined from the earliest date possible.

3) T. YUKUTAKE and H. TACHINAKA, "The Non-dipole Part of the Earth's Magnetic Field," *Bull. Earthq. Res. Inst.*, **46** (1968), 1027-1074.

4) K. WHITHAM, "The Relationships between the Secular Change and the Non-dipole Fields," *Canad. Jour. Phys.*, **3** (1958), 3-27.

5) *loc. cit.*, 2).

6) V. I. POCHTAREV, "The Western Drift of the Geomagnetic Field," *Geomag. Aeron.*, **4** (1964), 289-291 (English).

7) T. YUKUTAKE, "The Westward Drift of the Earth's Magnetic Field in Historic Times," *Jour. Geomag. Geoelectr.*, **19** (1967), 103-116.

2. Spherical harmonic coefficients for the geomagnetic secular change

Analyses of the geomagnetic secular change have so far been based on the observation at permanent stations. Mean rates of change in the field components over a decade or so have been computed at each station and then analysed to give a set of spherical harmonic coefficients $(\dot{g}_n^m, \dot{h}_n^m)$ for the magnetic potential. Obviously this process requires a close network of well equipped observatories. This is the main reason why the spherical harmonic analyses of the secular change we have are limited to the 20th century data.

However, it is theoretically possible to obtain the harmonic coefficients of the secular change from those of the main field (g_n^m, h_n^m) analysed for different epochs. If the coefficients of the main field are accurate enough, differences between corresponding coefficients for different epochs give the amount of change in the magnetic potential in the interval. This method, however, has been paid little regard so far, probably because the data of magnetic surveys or those at the repeat stations on which the analyses of the main field are mostly based can hardly get rid of errors contracted from local anomalies at the observation points or magnetic disturbances of external origin such as magnetic storms or diurnal variations, which are sometimes much larger than the annual mean rate of change to be obtained.

The accuracy of the spherical harmonic analyses of the main field was discussed in a previous paper[8], in which the spherical harmonic coefficients of different analyses for the same epoch were compared. For the higher harmonics, the diffierences between the corresponding terms become the same order of magnitude with the harmonic coefficients themselves, suggesting that either of the analyses is erroneous for the harmonic coefficient concerned. Comparing the analysis by Fanselau and Kautzleben whith that by Vestine et al. which are based on the same materials for 1945, $|\Delta g_n^m|/C_n^m$ and $|\Delta h_n^m|/C_n^m$ were computed, where Δg_n^m and Δh_n^m are the differences between the corresponding Gauss-Schmidt coefficients and $C_n^m=\sqrt{(g_n^m)^2+(h_n^m)^2}$. The results indicate a kind of error level for individual coefficients. Fig. 1 thus obtained shows that the differences become comparable with the primary coefficients only for the terms $n=6$, $m=4$ and $n=6$, $m=6$.

Differences of the corresponding terms between Leaton et al.'s

8) T. YUKUTAKE, "Synthesis of the Non-dipole Components of the Earth's Magnetic Field from Spherical Harmonic Coefficients," *Bull. Earthq. Res. Inst.*, **46** (1968), 385-403.

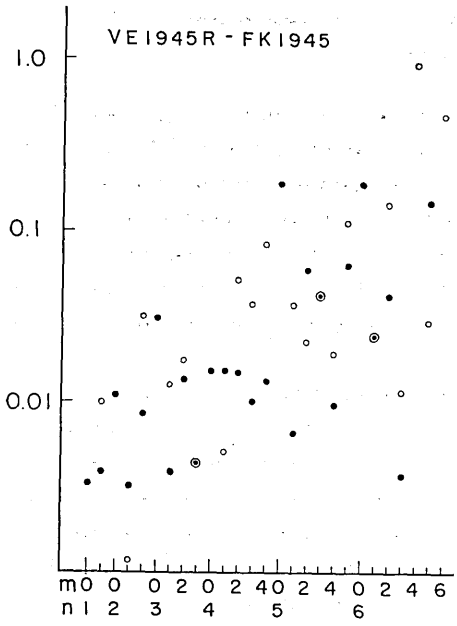

Fig. 1. Discrepancies between two sets of Gauss-Schmidt coefficients for the same epoch 1945. Fanselau-Kautzleben's analysis is compared with that of Vestine et al. Solid circles denote $|\Delta g_n^m|/C_n^m$ and hollow circles $|\Delta h_n^m|/C_n^m$. This provides a kind of error level when the rate of change in the harmonic coefficients is computed from the difference between coefficients of different epochs.

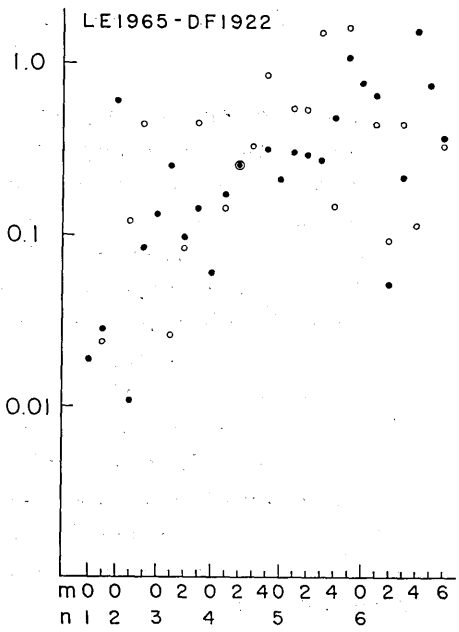

Fig. 2. $|\Delta g_n^m|/C_n^m$ (solid circles) and $|\Delta h_n^m|/C_n^m$ (hollow circles) obtained by comparing Leaton et al.'s analysis for 1965 with Dyson-Furner's for 1922. Values of $|\Delta g_n^m|/C_n^m$ and $|\Delta h_n^m|/C_n^m$ are larger than those of Fig. 1, indicating that the differences between the two analysis are beyond the errors included in the analyses.

analysis for 1965 and Dyson and Furner's for 1922 were computed and $|\Delta g_n^m|/C_n^m$ and $|\Delta h_n^m|/C_n^m$ are shown in Fig. 2. It shows that, for all the harmonics, $|\Delta g_n^m|/C_n^m$ and $|\Delta h_n^m|/C_n^m$ calculated for Leaton et al.'s and Dyson-Furner's analysis exceed the error levels shown in Fig. 1. In Table 1, harmonic coefficients for the secular change for 1943.5 computed from the differences between Leaton et al.'s and Dyson-Furner's analysis are tabulated together with a few analyses of the secular change based on the observatory data. In the second columm, the ratios (k_n^m) of $|\Delta g_n^m|/C_n^m$ (or $|\Delta h_n^m|/C_n^m$) calculated from Leaton et al.'s and Dyson-Furner's analyses to that obtained by comparison of Vestine et al.'s and Fanselau-Kautzleben's analysis are shown. Almost all the k_n^m are much larger than

Table 1. The rate of change in the spherical harmonic coefficients of the main field for 1943.5 and the harmonic coefficients of the observed secular change.

n	m	1943.5[a] $\frac{\Delta g_n^m}{\Delta t}$	1943.5[a] $\frac{\Delta h_n^m}{\Delta t}$	k_n^m for g_n^m	k_n^m for h_n^m	1932.5[b] $\dot{g}_n^m$	1932.5[b] $\dot{h}_n^m$	1942.5[b] $\dot{g}_n^m$	1942.5[b] $\dot{h}_n^m$	1957.5[c] $\dot{g}_n^m$	1957.5[c] $\dot{h}_n^m$
		γ/yr.	γ/yr.			γ/yr.	γ/yr.	γ/yr.	γ/yr.	γ/yr.	γ/yr.
1	0	13.4		5.7		23.0		9.2		13.6	
1	1	4.0	−3.5	7.1	2.4	1.3	−4.7	1.6	1.3	5.9	2.3
2	0	−17.7		54.6		−14.1		−17.9		−21.5	
2	1	−0.9	−17.5	3.4	188.0	1.3	−17.6	0.1	−19.7	−1.8	−16.0
2	2	3.2	−16.9	9.9	14.2	9.8	−13.7	2.4	−14.2	−0.1	−17.1
3	0	3.4		4.3		4.2		1.8		1.9	
3	1	−10.8	1.1	65.2	2.1	−7.3	−5.2	−7.3	−0.6	−8.2	8.2
3	2	2.8	2.5	7.1	4.8	0.7	3.5	3.3	4.1	1.1	3.5
3	3	2.8	−8.9	32.4	102.0	3.1	−12.8	0.1	−10.4	−0.5	−6.7
4	0	1.3		4.0		4.8		4.6		−4.4	
4	1	3.1	−2.6	11.2	28.9	2.5	−4.3	1.5	−3.1	2.7	0.0
4	2	−3.7	−3.6	17.3	5.0	−2.7	−5.7	−1.0	−5.9	−2.0	−1.1
4	3	0.0	3.2	0.0	9.0	1.7	3.1	2.9	3.0	−1.0	3.5
4	4	2.0	−5.5	23.9	46.9	3.4	−3.4	2.6	−2.2	−2.2	−2.1
5	0	1.0		11.2		−2.1		−2.3		2.1	
5	1	2.3	4.1	45.8	15.0	−1.5	6.2	0.5	4.7	−1.8	1.8
5	2	1.6	2.9	5.0	23.7	−3.0	1.4	−1.6	2.0	0.2	1.7
5	3	0.5	−3.0	6.5	36.0	−0.6	−0.5	−0.2	−0.9	1.0	−3.8
5	4	−2.0	0.6	51.0	7.8	−2.2	0.1	−0.7	0.0	−0.5	0.7
5	5	−1.5	2.3	17.2	14.8	−1.9	2.8	−1.4	3.0	−0.2	0.2
6	0	−1.2		4.1		0.7		2.3		−1.7	
6	1	1.3	−0.9	26.9	18.6	1.4	−1.8	−0.2	−1.9	2.1	−0.7
6	2	0.1	0.2	1.3	0.6	1.9	−0.1	1.3	0.7	0.1	−0.2
6	3	−1.1	2.3	58.8	40.5	−1.1	0.4	−0.7	0.3	−0.3	1.5
6	4	1.9	−0.1	∞	0.1	1.3	1.0	1.0	0.0	1.5	−1.1
6	5	−0.5	−0.5	5.2	27.1	−0.9	−0.8	−1.4	−0.8	0.5	0.7
6	6	−0.8	0.8	∞	0.7	−1.8	1.6	−0.2	1.2	−0.6	1.0

a) Obtained from differences between Leaton et al.'s analysis for 1965 and Dyson and Furner's for 1922.

b) E. H. VESTINE, W. L. SIBLEY, J. W. KERN and J. L. CARLSTEDT, *Jour. Geomag. Geoelectr.*, **15** (1963), 47-72.

c) T. NAGATA and Y. SYONO, *Jour. Geomag. Geoelectr.*, **12** (1961), 84-98.

Table 2. Spherical harmonic coefficients of the geomagnetic secular variation.

n	m	1743		1806		1857		1900	
		$\dot{g}_n^m$	$\dot{h}_n^m$	$\dot{g}_n^m$	$\dot{h}_n^m$	$\dot{g}_n^m$	$\dot{h}_n^m$	$\dot{g}_n^m$	$\dot{h}_n^m$
		γ/yr.		γ/yr.		γ/yr.		γ/yr.	
1	0	2.1		−4.2		9.8		17.3	
1	1	0.4	16.5	22.7	19.9	11.9	−2.6	4.3	−0.6
2	0	0.1		3.2		−14.2		−12.2	
2	1	4.4	−7.2	8.9	−5.3	2.9	−15.7	2.0	−14.3
2	2	10.5	14.2	13.7	7.3	14.1	−0.9	17.6	−12.6
3	0	0.9		−5.0		10.7		0.9	
3	1	−3.8	0.7	−8.1	−0.7	−2.2	5.5	−7.2	−2.3
3	2	3.8	0.5	4.8	3.3	−0.3	−7.4	−4.2	1.7
3	3	0.5	3.7	13.4	5.3	7.0	−4.4	7.6	−9.3
4	0	0.6		7.2		1.0		1.9	
4	1	2.1	0.7	−3.5	3.9	−4.7	8.1	2.0	0.6
4	2	−0.1	1.3	2.4	−0.2	2.2	3.8	2.5	0.1
4	3	−2.3	−0.1	−2.3	2.2	0.8	−3.0	−2.5	1.7
4	4	0.0	0.3	−0.8	3.6	6.0	0.6	2.1	1.2
5	0							−1.8	
5	1							−1.2	3.0
5	2							−2.8	0.9
5	3							−1.2	0.1
5	4							−1.1	−1.3
5	5							−2.0	−0.3
6	0							0.6	
6	1							0.4	−0.8
6	2							1.2	0.8
6	3							−1.3	0.4
6	4							−0.2	0.1
6	5							0.1	−1.2
6	6							−1.3	−0.8

unity. It means that the harmonic coefficients of the secular variation can be determined beyond the errors included in the main field analyses. Consistency of the results with the other analyses based on the observed rate of change in the magnetic elements at permanent observatories in Table 1 also confirms the validity of the present method.

Following the same procedure, examination of the error levels for

the harmonic coefficients of the main field analyses were carried out for different epochs[9]. It followed that for the 20th century data the coefficients up to $n=6$, $m=6$ could be used for the present purpose, and for the 19th century data those up to $n=4$, $m=4$. The result suggests that we can obtain sufficiently reliable coefficients of the secular change by this method provided the main field analyses are taken at appropriate intervals.

In this way, the harmonic coefficients of the geomagnetic secular variations were computed for 1806, 1857 and 1900. They are listed in Table 2, together with the coefficients for 1743 obtained by Fritsche following the similar procedure[10]. A brief description is given below about the process of obtaining the respective sets of harmonic coefficients.

1743 data—Based on his own analyses of the main field, Fritsche first averaged the corresponding terms for 1600, 1650 and 1700, to give the mean harmonic coefficients for the epoch 1650. Similarly for 1780, 1842 and 1885 analyses, he calculated the mean coefficients for 1836, then computed the secular variation in the harmonic coefficients during the period from 1650 to 1836. In this paper, the amount of change thus obtained was simply divided by the interval 186 years to give the mean rate of change in the harmonic coefficients.

1806 data—Main field analyses for 1780 by Fritsche and Carlheim-Gyllensköld were combined with those for 1829 by Erman and Petersen and for 1935 by Gauss to obtain the secular change for 1804.5 and 1807.5 as follows.

FR 1780[11]—EP 1829[11]	SV 1804.5	SV 1806[11]
FR 1780 —GA 1835[11]	SV 1804.5	
CG 1780 —EP 1829	SV 1804.5	
CG 1780 —GA 1835	SV 1807.5	

9) *loc. cit.*, 8)

10) H. FRITSCHE, *Die Elemente des Erdmagnetismus für die Epochen 1600, 1650, 1700, 1780, 1842 und 1885, und Ihre Saecularen Aenderungen*, (St. Petersburg 1899).

11) Abbreviations used are as follows

F R 1780, F R 1885: Fritsche's main field analyses for 1780 and 1885.
C G 1780: Carlheim-Gyllensköld's main field analysis for 1780.
E P 1829: Erman and Petersen's main field analysis for 1829.
G A 1835: Gauss' main field analysis for 1835.
A D 1845, A D 1880: Adams' main field analyses for 1845 and 1880.
N P 1885: Neumayer and Petersen's main field analysis for 1885.
S C 1885: Schmidt's main field analysis for 1885.
D F 1922: Dyson and Furner's main field analysis for 1922.
V E 1945: Vestine et al.'s main field analysis for 1945.
F L 1955: Finch and Leaton's main field analysis for 1955.
S V 1806: A set of spherical harmonic coefficients of the secular variation for 1806.

The harmonic coefficients for 1806 were then calculated by averaging the secular change coefficients for 1804.5 ahd 1807.5.

1857 data—Erman-Petersen's 1829 analysis and Gauss' 1835 analysis were combined with Neumayer-Petersen's analysis for 1885, Schmidt's 1885, Fritsche's 1885 and Adams' 1880 analysis. Averaging the secular variation coefficients obtained from various combinations of the above main field analyses, the harmonic coefficients of the secular change were obtained as follows.

EP 1829—NP 1885[11]	SV 1857.0	SV 1857
EP 1829—SC 1885[11]		
EP 1829—FR 1885		
GA 1835—NP 1885	SV 1860.0	
GA 1835—SC 1885		
GA 1835—FR 1885		
EP 1829—AD 1880[11]	SV 1854.5	
GA 1835—AD 1880[11]	SV 1857.5	

1900 data—Adams' analyses for 1845 and 1880 and the analyses for 1885 by Neumayer-Petersen, Schmidt and Fritsche were compared with Dyson-Furner's 1922 analysis, Vestine et al.'s 1945 and Finch-Leaton's 1955 analysis. Averaging the secular variation coefficients thus calculated for 1900.0, 1895.0, 1901.0 and 1903.5, the 1900 data were obtained.

AD 1845—FL 1955	SV 1900.0	SV 1900
AD 1845—VE 1945	SV 1895.0	
AD 1880—DF 1922	SV 1901.0	
NP 1885—DF 1922	SV 1903.5	
SC 1885—DF 1922		
FR 1885—DF 1922		

Besides these sets of spherical harmonic coefficients of the geomagnetic secular change, we have employed for this study the analyses by Vestine et al.'s for 1942.5[12] and by Leaton et al.'s for 1965[13].

3. The rate of change in the non-dipole field

Rates of change in the non-dipole parts of the earth's magnetic

12) E. H. VESTINE, W. L. SIBLEY, J. W. KERN and J. L. CARLSTEDT, "Integral and Spherical Harmonic Analyses of the Geomagnetic Field for 1955.0, Part 1," *Jour. Geomag. Geoelectr.*, **15** (1963), 47-72.

13) B. R. LEATON, S. R. C. MALIN and M. J. EVANS, "An Analytical Representation of the Estimated Geomagnetic Field and Its Secular Change for the Epoch 1965. 0," *Jour. Geomag. Geoelectr.*, **17** (1965), 187-194.

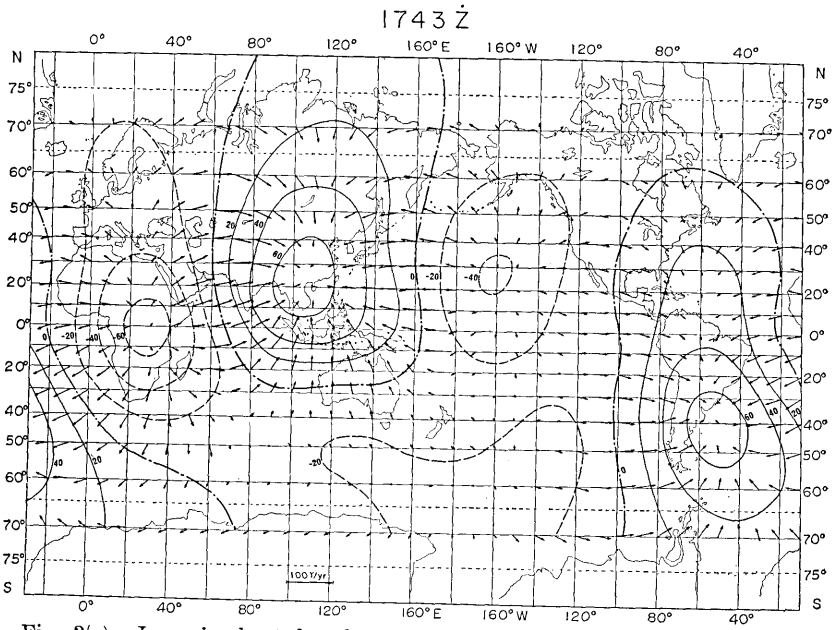

Fig. 3(a). Isoporic chart for the non-dipole vertical component for 1743.

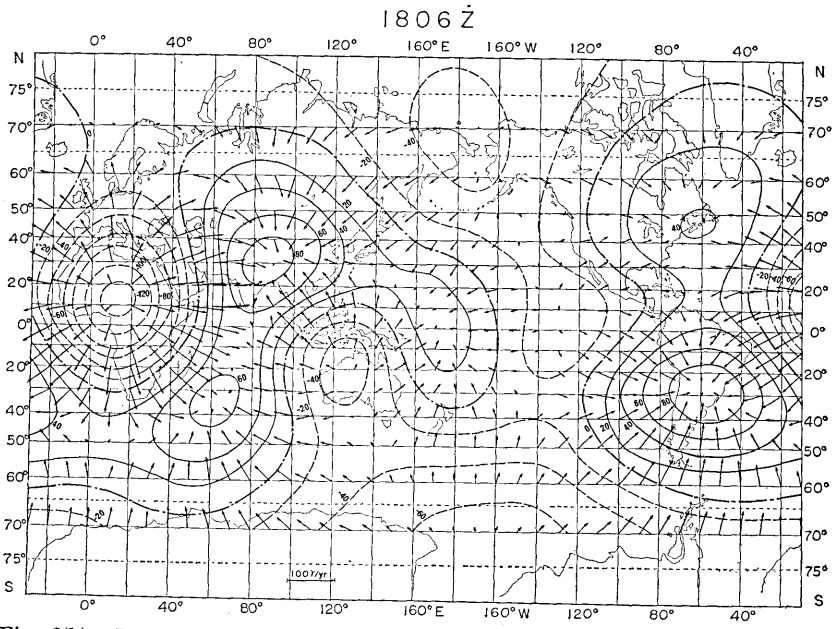

Fig. 3(b). Isoporic chart for the non-dipole vertical component for 1806. The contours give the rate of change in the vertical component at intervals of 20γ/year. The arrows give the rate of change in the horizontal component.

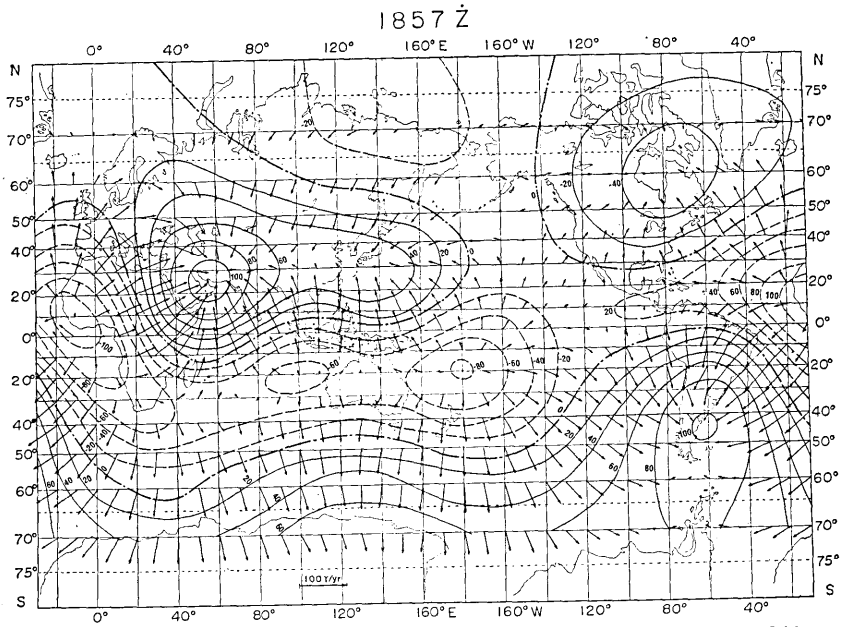

Fig. 3(c). Isoporic chart for the non-dipole vertical component for 1857.

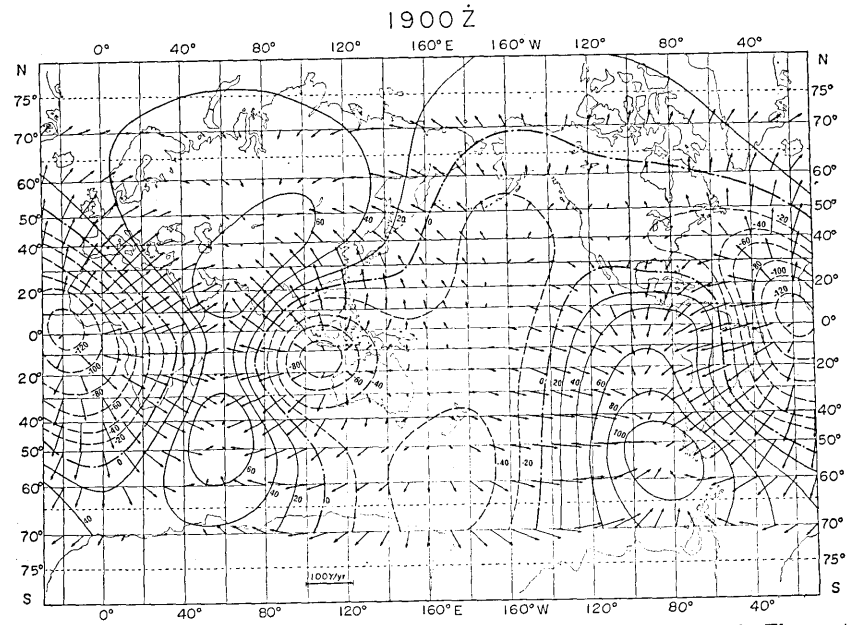

Fig. 3(d). Isoporic chart for the nondipole vertical component for 1900. The contours give the rate of change in the vertical component at intervals of 20γ/year. The arrows give the rate of change in the horizontal component.

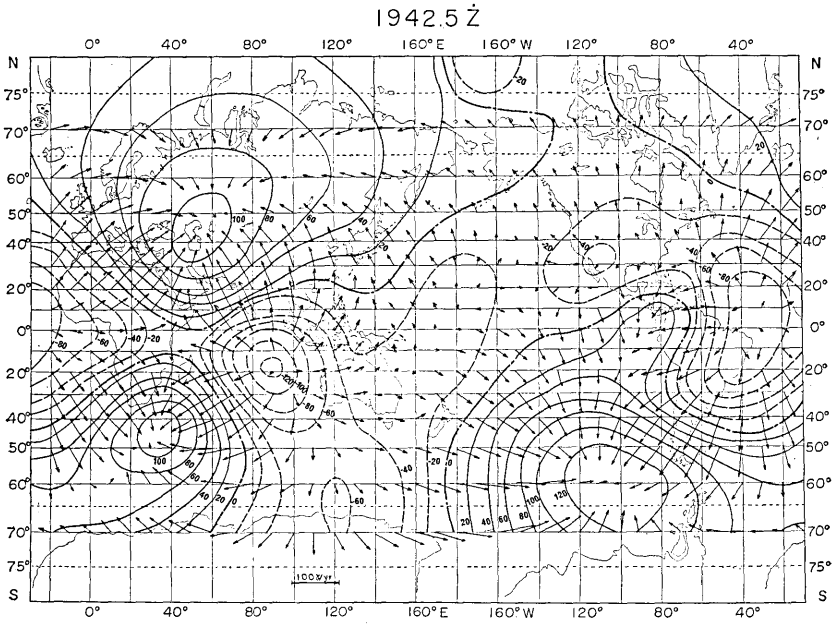

Fig. 3(e). Isopolic chart for the non-dipole vertical component for 1942.5.

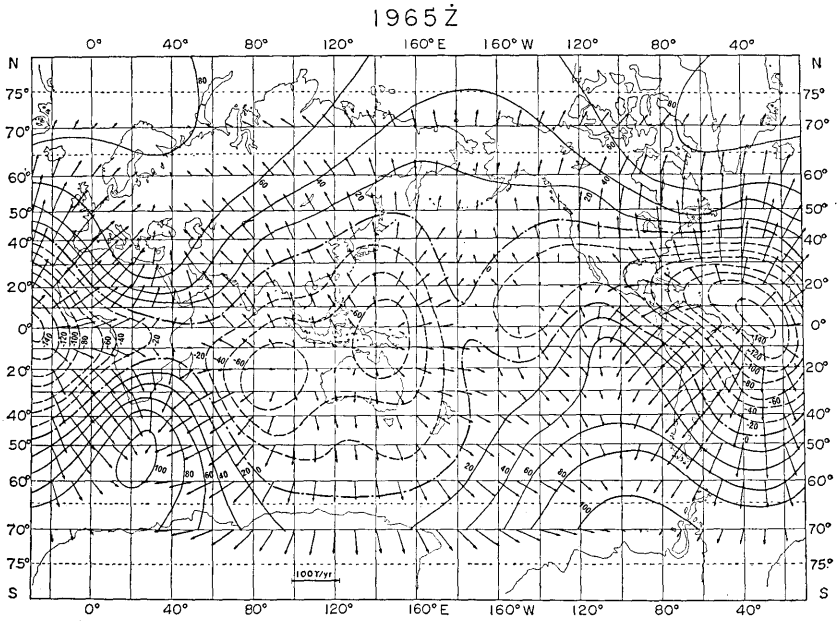

Fig. 3(f). Isoporic chart for the non-dipole vertical component for 1965. The contours give the rate of change in the vertical component at intervals of 20γ/year. The arrows give the rate of change in the horizontal component.

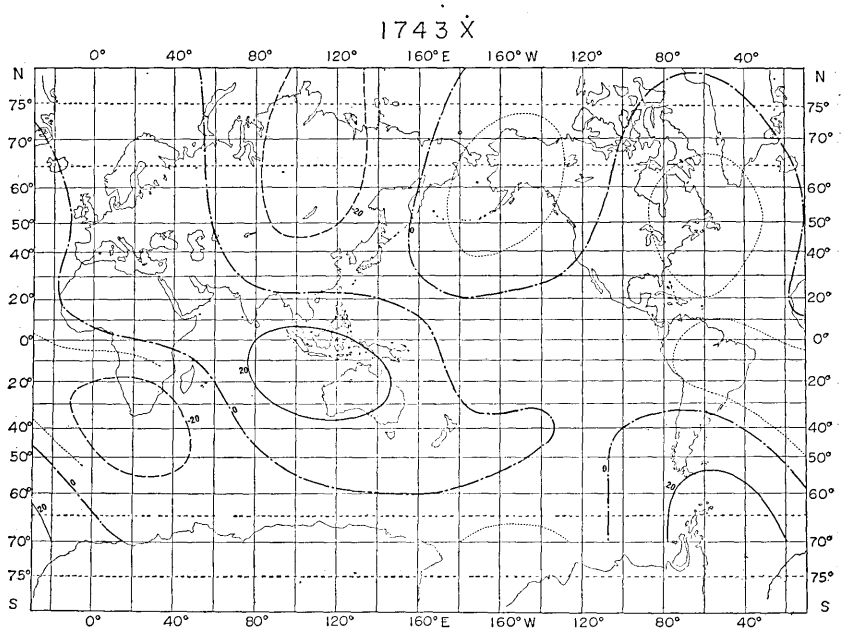

Fig. 4(a). Isoporic chart for the non-dipole north component for 1743, contour interval 20γ/year.

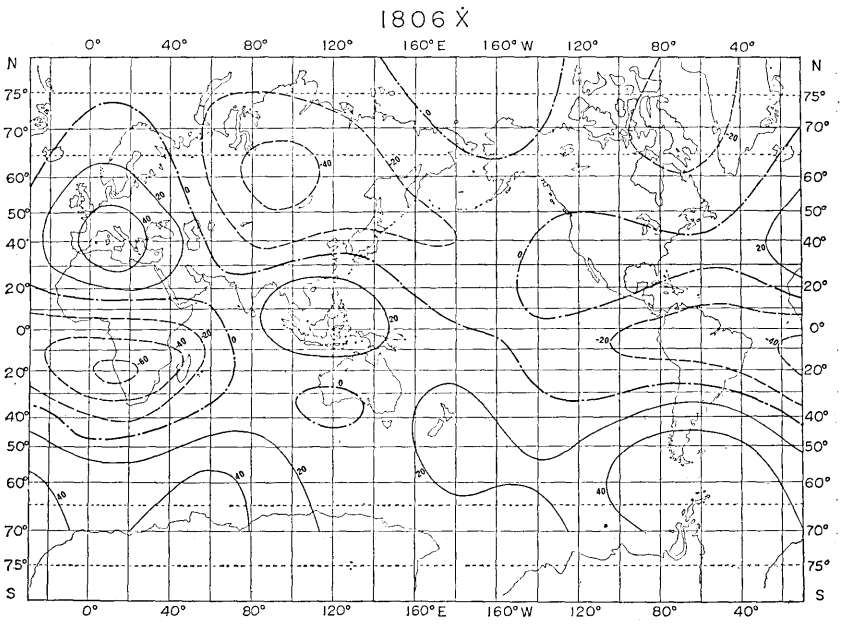

Fig. 4(b). Isoporic chart for the non-dipole north component for 1806, contour interval 20γ/year.

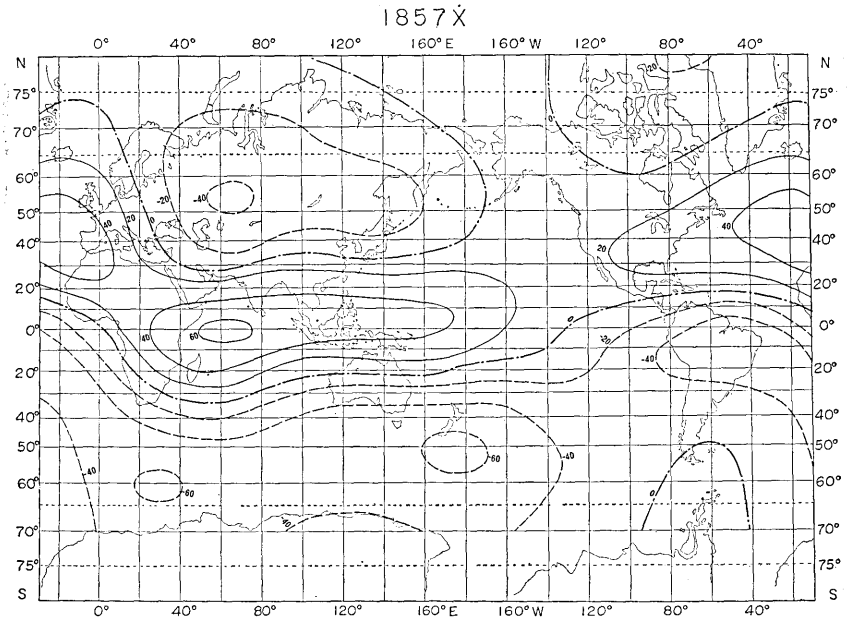

Fig. 4(c). Isoporic chart for the non-dipole north component for 1857, contour interval 20γ/year.

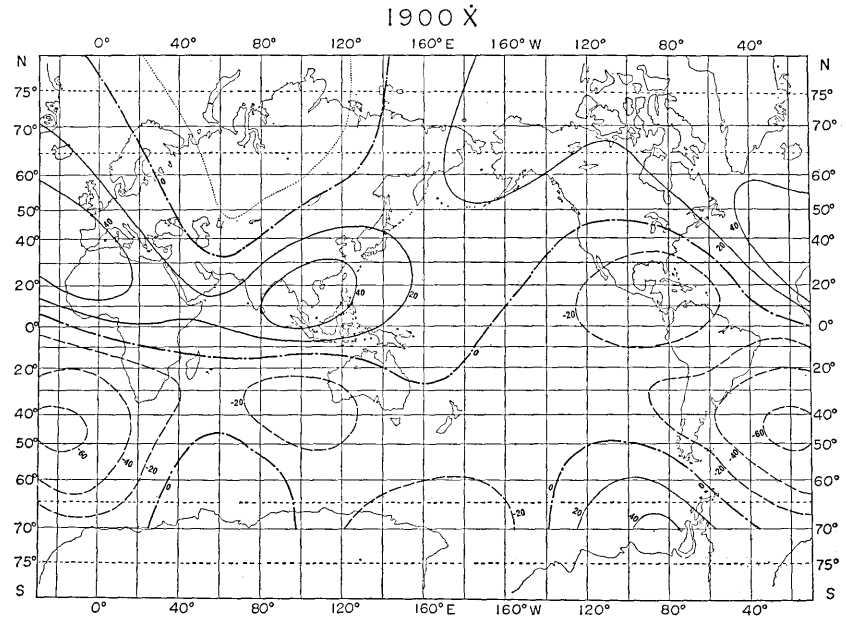

Fig. 4(d). Isoporic chart for the non-dipole north component for 1900, contour interval 20γ/year.

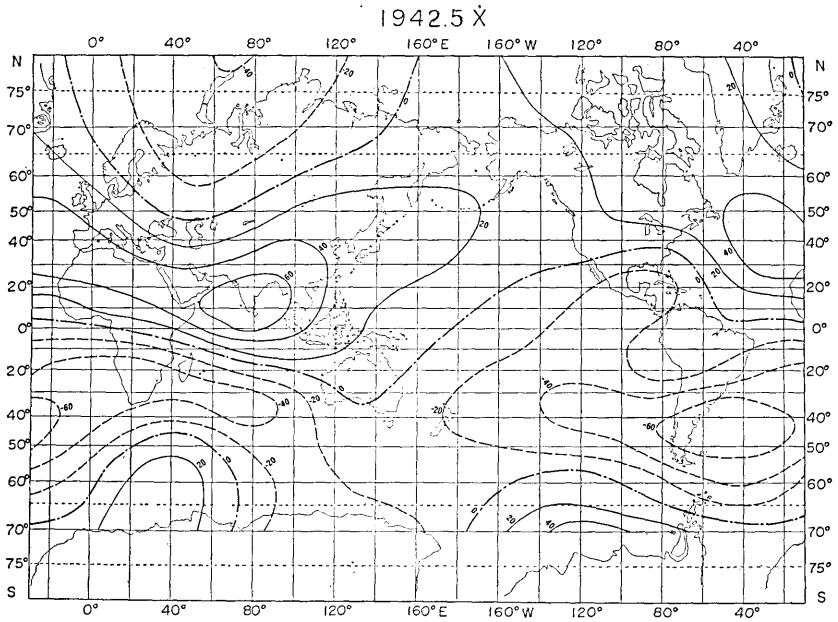

Fig. 4(e). Isoporic chart for the non-dipole north component for 1942.5, contour interval 20γ/year.

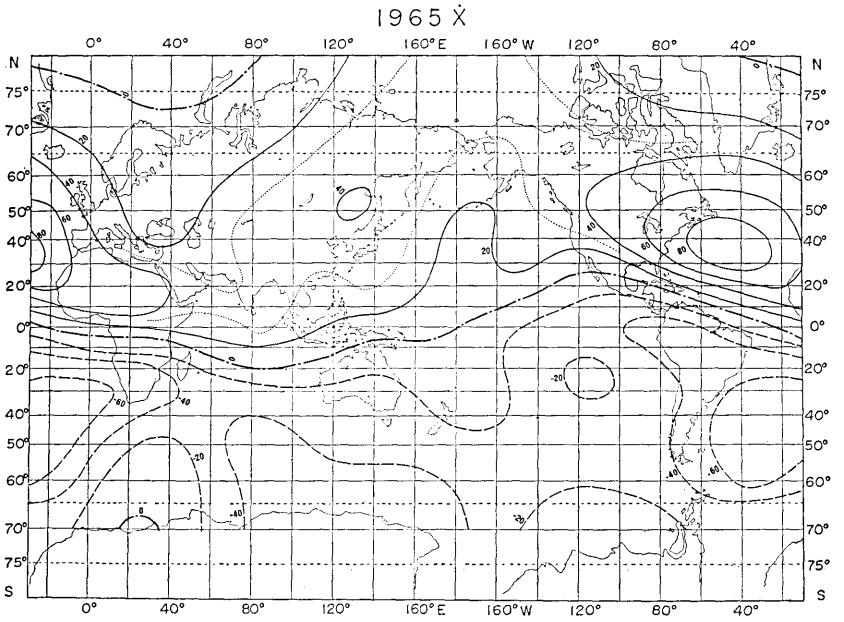

Fig. 4(f). Isoporic chart for the non-dipole north component for 1965, contour interval 20γ/year.

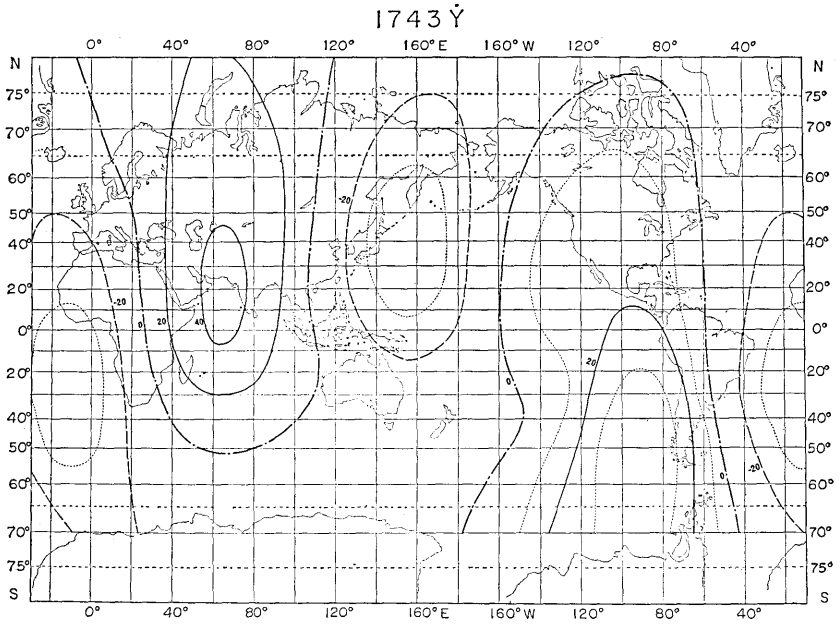

Fig. 5(a). Isoporic chart for the non-dipole east component for 1743, contour interval 20γ/year.

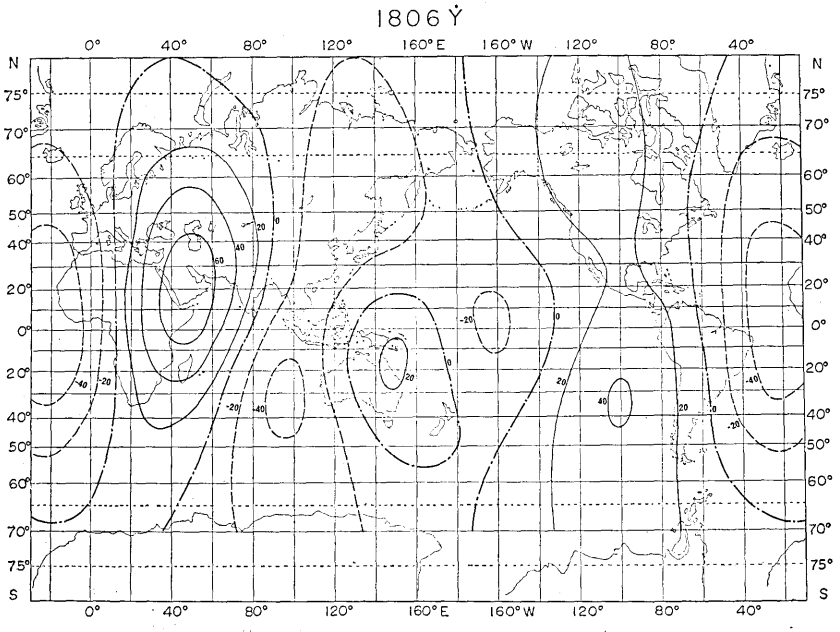

Fig. 5(b). Isoporic chart for the non-dipole east component for 1806, contour interval 20γ/year.

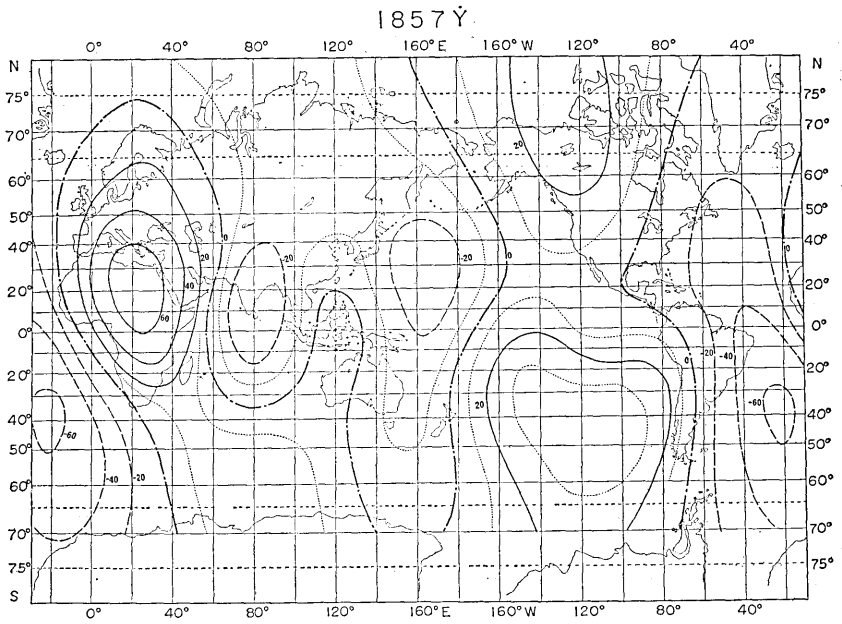

Fig. 5(c). Isoporic chart for the non-dipole east component for 1857, contour interval 20γ/year.

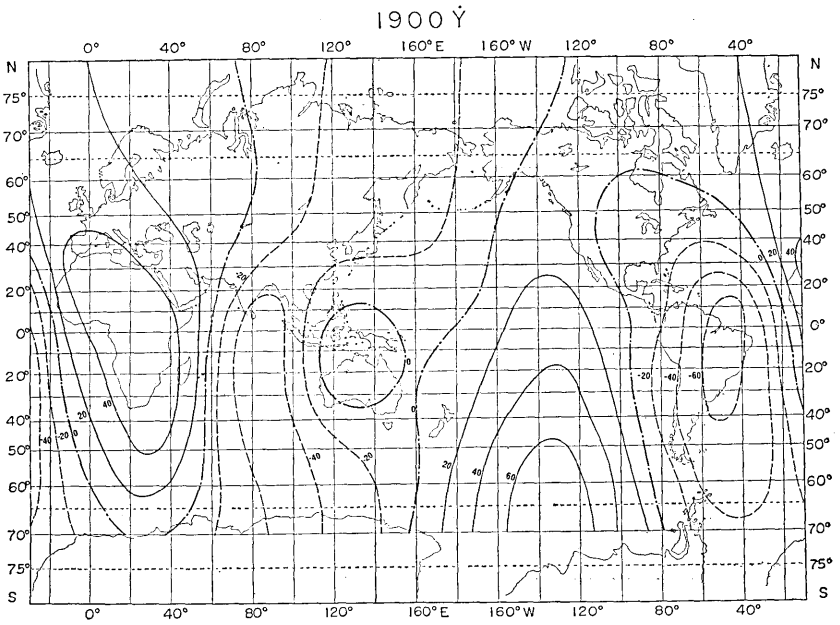

Fig. 5(d). Isoporic chart for the non-dipole east component for 1900, contour interval 20γ/year.

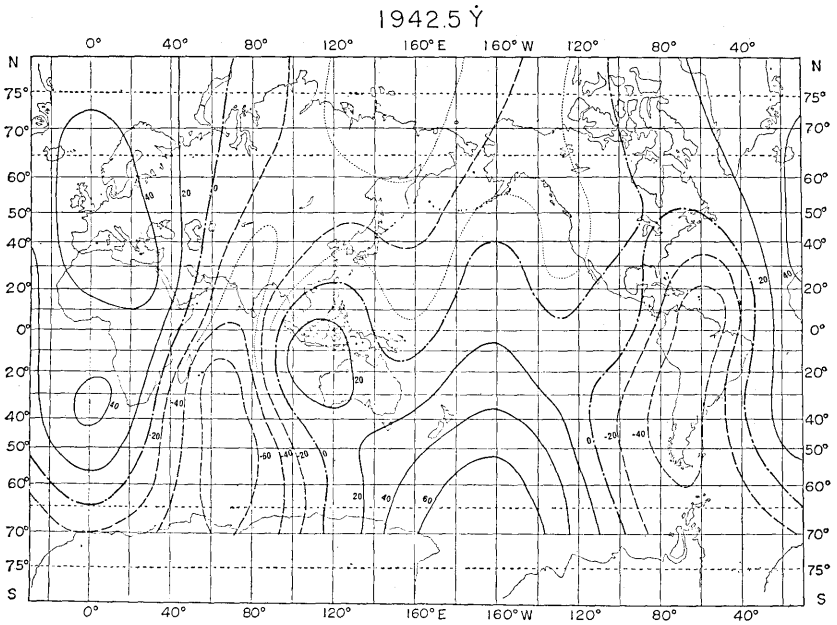

Fig. 5(e). Isoporic chart for the non-dipole east component for 1942.5, contour interval 20γ/year.

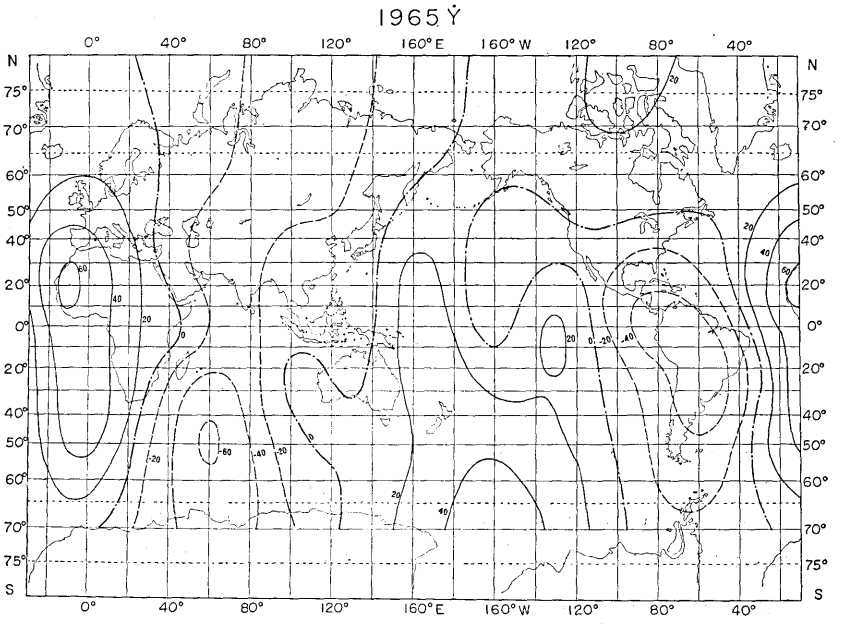

Fig. 5(f). Isoporic chart for the non-dipole east component for 1965, contour interval 20γ/year.

field are synthesized from the spherical harmonic coefficients $(\dot{g}_n^m, \dot{h}_n^m)$ for the geomagnetic secular change as follows,

$$\dot{X}=\sum_{n=2}^{N}\sum_{m=0}^{n}(\dot{g}_n^m\cos m\lambda+\dot{h}_n^m\sin m\lambda)\frac{dP_n^m(\theta)}{d\theta},$$

$$\dot{Y}=-\frac{1}{\sin\theta}\sum_{n=2}^{N}\sum_{m=0}^{n}m(-\dot{g}_n^m\sin m\lambda+\dot{h}_n^m\cos m\lambda)P_n^m(\theta),$$

$$\dot{Z}=-\sum_{n=2}^{N}(n+1)\sum_{m=0}^{n}(\dot{g}_n^m\cos m\lambda+\dot{h}_n^m\sin m\lambda)P_n^m(\theta),$$

where $\dot{X}$, $\dot{Y}$ and $\dot{Z}$ are the rates of change in the north, the east and the vertical downward component of the non-dipole field respectively. $P_n^m(\theta)$ is Schmidt's half-normalized spherical function of degree n and order m, and N is the maximum degree employed for the analysis. θ and λ denote the colatitude and the east longitude. Figs. 3 to 5 show the distributions of rate of change (isoporic charts) in the vertical force, the northerly force and the easterly force for various epochs.

3-1. *The westward drift of the isoporic foci*

Figs. 3(a) to (f) are isoporic charts for the vertical component of the non-dipole field for 1743, 1806, 1857, 1900, 1942.5 and 1965. Although several foci cover the whole surface of the earth as well as the regional anomalies of the non-dipole field do, it may be noticed that the isoporic foci distribute more regularly than the non-dipole field itself[14]. In Fig. 3(b), showing 1806 isoporic chart, for example, a few negative foci align in the low latitudes along the equator. Positive foci form pairs in the meridional direction at about 80°E and 60°W, each focus of the pair being situated in the middle latitude near 40° north and south. It is also remarkable that the pairs of the positive foci and the negative ones distribute alternately in the east west direction.

It has been widely believed that the isoporic foci are very short lived and probably disappear within a hundred years. However, we can trace the vicissitudes of individual foci during the past few hundred years in Figs. 3(a) to (f), indicating that the life of an isoporic focus is much longer than has been assumed. When the locations of individual foci are examined from 1743 to 1965, the westward drifting

14) Compare with the non-dipole charts in:
T. YUKUTAKE and H. TACHINAKA, "The Non-dipole Part of the Earth's Magnetic Field," *Bull. Earthq. Res. Inst.*, **46** (1968), 1027-1074.

is obviously noted for all the foci. It should be compared with the observational result regarding the non-dipole field that the considerable part of the regional anomalies has been standing still nearly at the same place during the period[15]. In Fig. 6, locations of several conspicuous foci for various epochs are plotted. From these, drift velocities of foci are estimated to range from 0.22°/year to 0.32°/year.

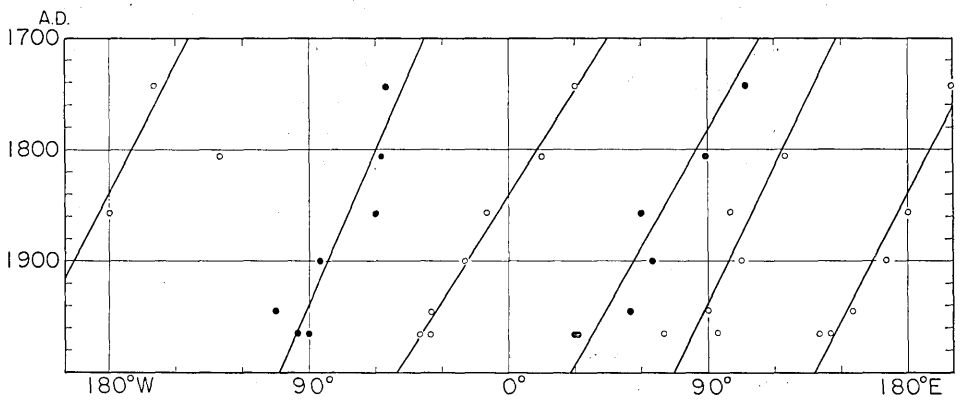

Fig. 6. Westward drift of isoporic foci for the vertical component. The longitudes of the foci are plotted for several epochs. Solid circles denote the locations of positive foci, and open ones those of negative foci. From right to left, a negative focus covering New Guinea, a negative one in the Indian Ocean, a positive focus over the Middle East, a negative in the Atlantic and a positive focus in the Pacific-Antarctic as of 1965.

The westward drift of the secular change can be more clearly seen when the profiles along a parallel circle are compared for various epochs. Figs. 7(a) to (c) show distributions of the secular change in the vertical component of the non-dipole field along the parallel circles of 40°N, the equator and 20°S, and Figs. 8 and 9 the distributions of the rate of change in the north and the east component. In Fig. 7(a), there were two maxima in $\dot{Z}$ in 1743. Both proceeded westerly from 1743 to 1965, though the east maximum has become small and hard to discern. The west maximum gives the drift velocity of 0.29°/year. It should be remembered here that there exist two large positive anomalies in the non-dipole field around 40°N, one being the Mongolian positive anomaly and the other the North American positive one. They have been standing at the same locality during the last hundreds of years and no appreciable

15) *loc. cit.*, 14)

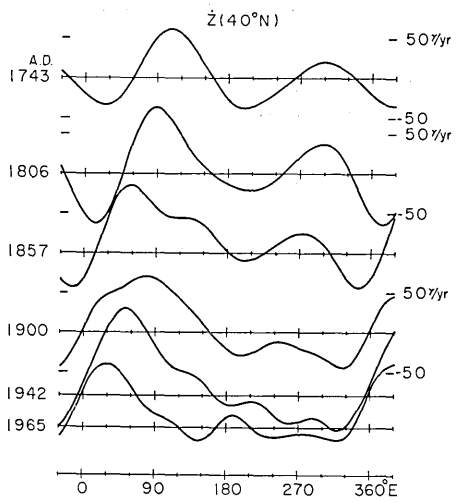

Fig. 7(a). The rate of change in the non-dipole vertical component along 40°N circle.

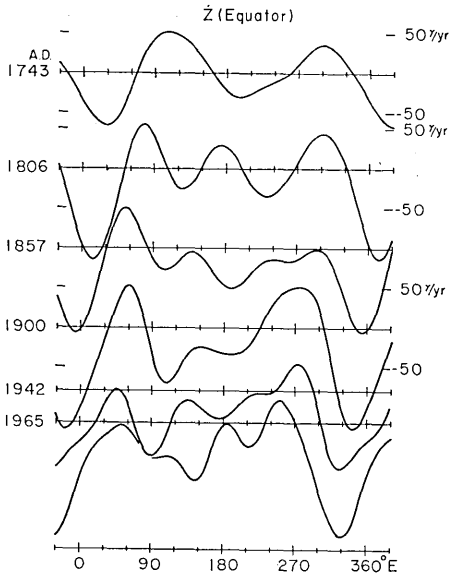

Fig. 7(b). The rate of change in the non-dipole vertical component along the equator.

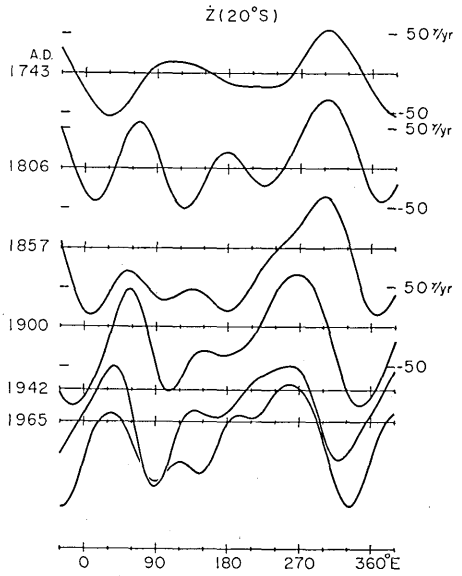

Fig. 7(c). The rate of change in the non-dipole vertical component along 20°S circle.

Fig. 7. Profiles of the rate of change in the non-dipole vertical component along parallels for various epochs. Distances between the zero lines for different epochs are taken nearly in proportion to the corresponding time interval.

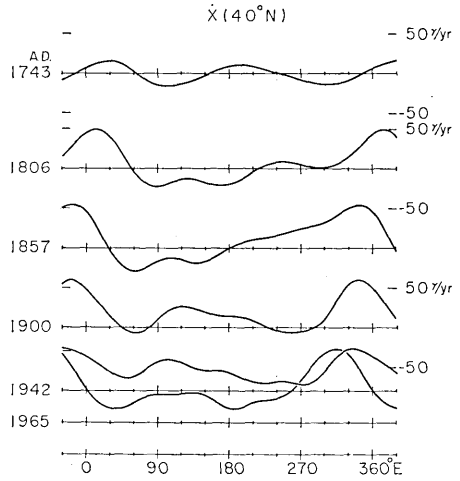

Fig. 8(a). The rate of change in the non-dipole north component along 40°N circle.

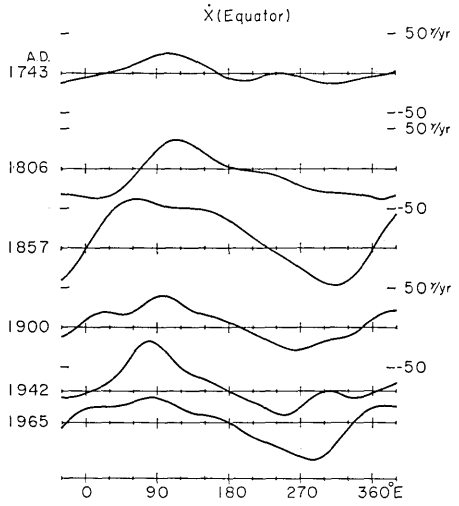

Fig. 8(b). The rate of change in the non-dipole north component along the equator.

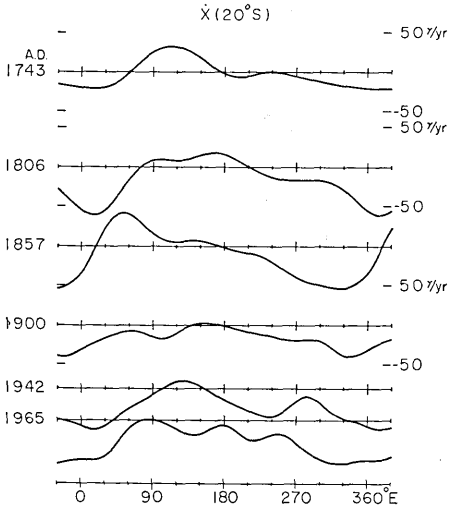

Fig. 8(c). The rate of change in the non-dipole north component along 20°S circle.

Fig. 8. Profiles of the rate of change in the non-dipole north component along parallels for various epochs. Distances between the zero lines for different epochs are taken nearly in proportion to the corresponding time interval.

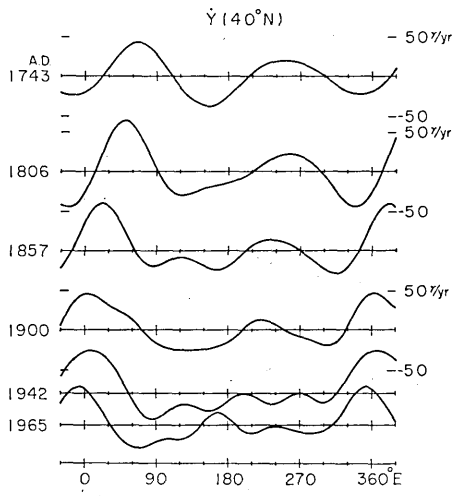

Fig. 9(a). The rate of change in the non-dipole east component along 40°N circle.

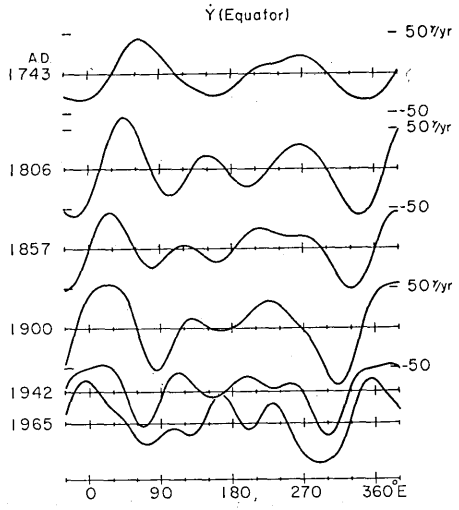

Fig. 9(b). The rate of change in the non-dipole east component along the equator.

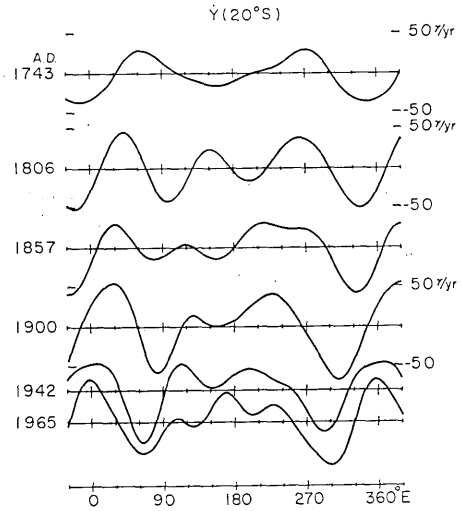

Fig. 9(c). The rate of change in the non-dipole east component along 20°S circle.

Fig. 9. Profiles of the rate of change in the non-dipole east component along parallels for various epochs. Distances between the zero lines for different epochs are taken nearly in proportion to the corresponding time interval.

drift has been observed along the 40°N parallel[16]. However, Fig. 7(a) indicates that, when the rate of change in the non-dipole field is taken, the effect of the standing anomaly becomes imperceptible and that the drifting part dominates the major behaviour of the secular change.

For $\dot{Z}$ along the equator in Fig. 7(b), we note a sharp negative with the minimum at about 30°E in 1743, which is supposed to be associated with the drifting African negative anomaly of the non-dipole field. It has moved westwards with a velocity of 0.30°/year. There are two positives on the equator situated near 100°E and 270°E in 1743, which also show westward travelling with similar velocities of 0.24°/year. For $\dot{Z}$ along 20°S, the main features are nearly the same as for along the equator.

For the rate of change in the north component, the effect of the westward drift is seen the least, because the isodynamic lines of the non-dipole field for the north component tend to run in the east west direction, which is, as can be easily understood, the most unfavourable for detecting the effect of westward drift. However, we can still notice the westward drift in $\dot{X}$ and that it is the most dominating feature in the secular change.

Fig. 9(a) shows the rate of change in the east component along the parallel circle of 40°N. It is clearly seen in the figure that two positive variations were located at about 60°E and 255°E in 1743 and that they have travelled westwards. As in the case of the rate of change in the vertical force, the positive variation near 255°E has decreased its amplitude. The drift velocity of the positive near 60°E is estimated to be 0.34°/year from the figure. As for the profiles along the equator and the 20°S parallel, the main features being well preserved during the period from 1743 to 1965, the westward drift plays the most important role in producing the observed distributions of the rate of change in the east component of the non-dipole field.

3-2. *Poleward shift of the isoporic foci*

Movement of the geomagnetic field in the meridional direction has been noted in terms of the northward shift of the eccentric dipole[17),18)].

16) *loc. cit.*, 14)

17) E. H. VESTINE, "On Variations of the Geomagnetic Field, Fluid Motions and Rate of the Earth's Rotation," *Jour. Geophys. Res.*, **58** (1953), 127-145.

18) T. NAGATA, "The Main Aspects of Geomagnetic Secular Variation—Westward Drift and Non-drifting Components," *Proc. Benedum Earth Magnetism Symp.*, (1962), 39-55.

Nagata and Rikitake considered that this should be due to the hydromagnetic oscillation of an axial quadrupole[19]. As for the meridional motion of the regional anomalies, there has been no detailed examination. If any meridional motions are discriminated, they will provide important materials for the study of hydromagnetism in the earth's core.

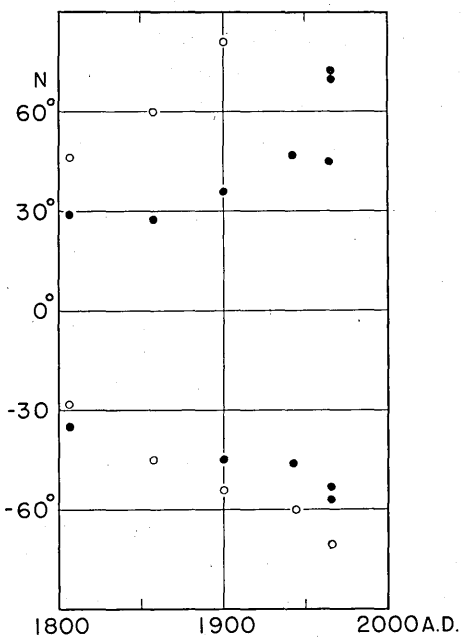

Fig. 10. Apparent poleward shift of the positive isoporic foci for the vertical force. The latitudes of two pairs of foci are plotted for several epochs. Solid circles represent the latitudes of a pair of foci situated near India in the 19th century, open ones those of foci over the American Continent. Apparent poleward velocity is about 0.14°/year for the Indian foci, and 0.26°/year for the American foci.

As has been already described, the pairs of positive foci of the vertical force located near 80°E and 300°E in 1806 have been moving westwards (Fig. 3). When the motions are examined more carefully, it may be noticed that each positive focus tends to depart from the equator and to proceed toward the poles. The latitudes of the centers of positive foci were read on the diagrams and plotted in Fig. 10. Solid circles represent the latitudes of the pair of foci situated near India (80°E) in 1806, and open ones those of positive foci near the American Continent (300°E) in 1806. Apparently poleward motions are recognized for these pairs of positive foci. The mean velocities were estimated to

19) T. NAGATA and T. RIKITAKE, "The Northward Shifting of the Geomagnetic Dipole and Stability of the Axial Magnetic Quadrupole of the Earth," *Jour. Geomag. Geoelectr.*, **14** (1963), 213-220.

be 0.14°/year for the Indian pair and 0.26°/year for the American pair.

It is rather supprising that the velocity of the poleward motion is nearly the same as that of the westward rotation, because none of the existing theory suggests that the radial velocity, which appears to be of the same order of magnitude as the meridional motion, can be larger than a tenth of the westward drift velocity[20),21)]. There is no sufficient data as yet to decide whether or not the substantial fluid motion toward the poles is really taking place in the core with the velocity indicated here. However, the later study of the change in the zonal components of the geomagnetic secular variation seems to suggest that the poleward shift of the positive foci obtained above is rather an apparent phenomenon accompanying a rapid growth of negative zone along the equator. And the rapid change in the negative zone might be accounted for by such a hydromagnetic process as Nagata and Rikitake suggested.

3-3. *Negative zone along the equator*

Another conspicuous feature in the isoporic charts in Figs. 3(a) to (f) is a negative belt along the equator. All the negative foci for the vertical component are aligned along the equator. With the lapse of time, the belt has been widened and in 1965 almost all the area between 20°N and 20°S was covered with the negative rate of change. On the other hand, as the negative belt has expanded, the polar regions have been covered by positive changes. It means that the vertical upward field is generated along the equator and converges downward at the polar regions. This is very clearly expressed in the rapid change in the harmonic coefficient $\dot{g}_2^0$ as is shown in Fig. 11. It is highly probable that the rapid change in the zonal coefficient of the secular change has shifted the location of the maxima of the secular change toward the poles.

4. Geomagnetic secular changes and historic variations in declination

In the previous section, it has been revealed that individual features in the isoporic charts have been drifting westwards with nearly the same velocities. It follows that the westward drift of the non-dipole

20) E. C. BULLARD and H. GELLMAN, Homogeneous Dynamos and Terrestrial Magnetism," *Phil. Trans. Roy. Soc. London*, A, **247** (1954), 213-278.

21) R. HIDE, "The Hydrodynamics of the Earth's Core," in L. H. AHRENS, K. RANKAMA and S. K. RUNCORN (Editors), *Physics and Chemistry of the Earth*, **1** (1956, Pergamon, London), 94-137.

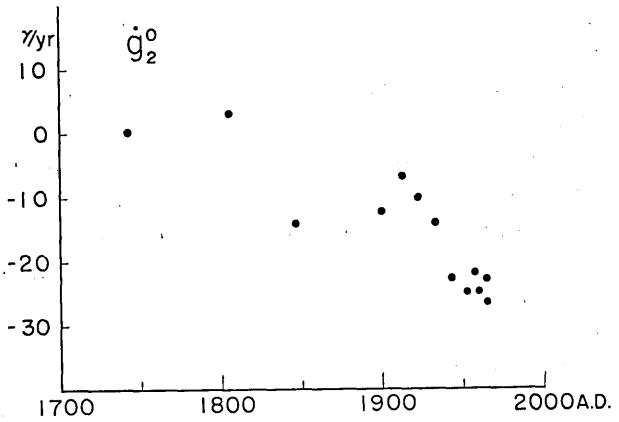

Fig. 11. Time variation in $\dot{g}_2^0$ for the past centuries.

field is not a local phenomenon restricted to such a specific region as off the coast of Guinea, but a phenomenon prevailing all over the world which is concealed in a certain area by predominant non-dipole anomalies that have been standing at the same locality.

The result that whole patterns of isopors are drifting seems in agreement with the westward drift of historic variations in the magnetic declination and inclination[22]. When the maximum deviations of declination or the maxima and the minima of inclination are examined, they exhibit a clear westward movement with nearly a constant velocity over several hundred years. Although the east component of the non-dipole field is not identical with the declination, the variation in the east component can be expected to be similar to that of the declination, because the variation in the declination is more dependent on that of the east component than on the north component. Therefore if the observed variations in declination and inclination are mainly due to the westward drift of the drifting anomalies, the longitudes, where the secular change in the east component becomes zero ($\dot{Y}=0$) for a certain epoch, give approximate places where the variation in the declination shows the maximum deviation.

Since most of the observation points for historic and archeomagnetic variation distribute in the middle latitude of the northern hemisphere, the longitudes of $\dot{Y}=0$ are read for the parallel circle 40°N (Fig. 5(a))

22) T. YUKUTAKE, "The Westward Drift of the Earth's Magnetic Field in Historic Times," *Jour. Geomag. Geoelectr.*, **19** (1967), 103-116.

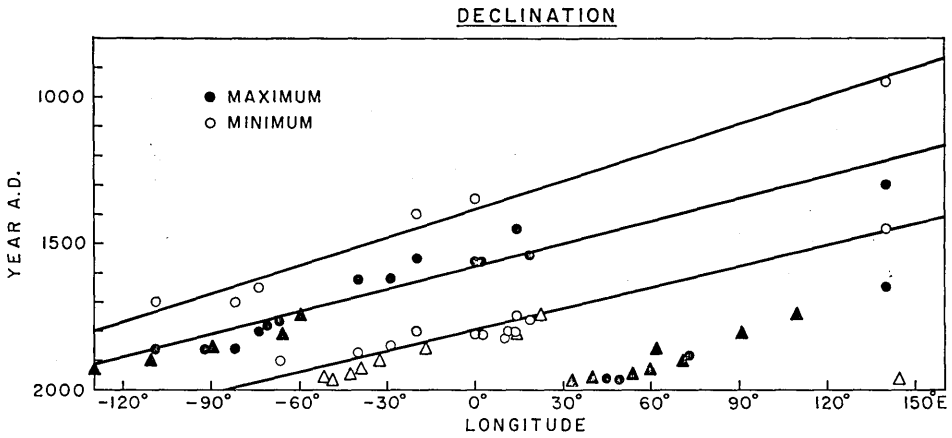

Fig. 12. Westward drift of the maximum deviations of magnetic declination. The epochs and the longitudes when and where the maximum deviations of declination were observed are designated by circles—solid for the maxima of easterly declination and open for the minima. Triangles were obtained from the reading of the longitude where the rate of change in the east component becomes zero ($\dot{Y}=0$) for various epochs. Triangles show a very good consistency with the historic declination data (circles).

and plotted in Fig. 12 by triangles where the solid ones denote the longitude and date of the maximum easterly component while the open ones those of the minimum. The westward drifts shown by triangles are in good agreement with those of circles obtained from historic records or archeomagnetic data, though the triangles cover only the recent portion of the historic variation. It may be concluded that the main feature of the secular variations even for historic times is due to the westward drift of the travelling parts of the non-dipole field.

---

52. 地球磁場経年変化の西方移動

地震研究所 {行武毅
立中ひろ子

地球磁場経年変化の解析は，固定観測所で観測された磁場の変化率をもととしてなされてきたが，理論的には主磁場解析より得られた球函数係数 (g_n^m, h_n^m) の時間変化を求めても同一の結果が得られる筈である．この方法を用いて，17 世紀以降の経年変化 ($\dot{g}_n^m, \dot{h}_n^m$) を推定し，非双極子部分の経年変化の時間的変動を調べた．

以上のようにして得られた経年変化の係数や，今世紀にはいってからの観測所の資料に基礎を置

く経年変化係数を合成して，地磁気3成分の経年変化分布を調べると，全体がほゞ一様な速度で過去200年間にわたって西方移動を続けてきたことがわかる．

一方，非双極子磁場それ自身は，大きな広がりをもつ数箇の磁気異常であるが，その大部分は同じ場所に停滞し，僅かに一つか二つの異常のみが西に移動していることが最近明かになった．しかし，経年変化の分布全体がほぼ一様に西方移動しているというこの研究の結果は，非双極子磁場中停滞している部分についても，それに重なりあって移動している部分のあることを示唆している．すなわち，非双極子磁場中移動するのは，ごく限られた狭い範囲の磁場分布でなく，全世界的広がりをもっていると考えられる．

また経年変化の分布をみると，時代とともに正の目玉が西方移動すると同時に極方向に位置を変えているのが認められる．